

Role of electron-phonon coupling on collision cascade development in Ni, Pd, and Pt

K. Nordlund,* L. Wei, Y. Zhong, and R. S. Averback
 Materials Research Laboratory, University of Illinois, Urbana, Illinois 61801
 (Received 12 March 1998)

Electron-phonon coupling in energetic collision cascades is believed to greatly enhance the cooling rate of heat spikes in many metals. Previous studies have not been able to conclusively determine the magnitude of the coupling, however. By directly comparing ion-beam mixing experiments and molecular dynamics simulations of collision cascades in Ni, Pd, and Pt metals, in which the coupling is believed to be most important, we show that the influence of electron-phonon coupling on mixing can be no more than about 30%, roughly an order of magnitude less than the most widely used models predict. [S0163-1829(98)53222-5]

The understanding of ion irradiation effects in solids has increased dramatically in recent years owing in large part to progress in computer simulations of energetic displacement cascades using molecular dynamics (MD).^{1,2} With the development of realistic interatomic potentials³⁻⁵ it is now possible to perform MD simulations of cascades in many semiconductors and metals.⁶⁻¹⁰ These potentials, however, are classical representations of atomic collisions in solids, and accordingly they neglect any possible coupling between the excited vibrational system of a material with the conduction electrons. In some important materials, such as Fe, Ni, Pd, and Pt, theoretical considerations suggest that electron-phonon coupling (EPC) should have a strong influence on cascade dynamics,¹¹⁻¹⁵ but unfortunately current theory is incapable of providing more than order-of-magnitude estimates of this effect.¹⁶ Some experimental work has also been focused on this question,^{17,18} but again without definitive conclusions. Since the conclusions of many recent and ongoing studies of energetic processes in metals depend critically on the effect of EPC on cascade dynamics (see, e.g., Refs. 12, 14, 15, and 19), the need for a reliable estimate of the magnitude of this effect is abundantly clear.

We present here a direct means of probing the magnitude of electron-phonon coupling through combined simulation and experimental studies. Quite simply, we compare experimental measurements of ion-beam mixing with calculations using molecular-dynamics simulations. The progress in this paper over all previous work is that by using a highly efficient MD code, we can now simulate displacement cascades with up to 200 keV of energy. This makes direct comparison with experimental studies possible. In the past, extrapolations of cascade effects were required from 20 keV to over 100 keV in order to access energy scales typical of actual experiments. We performed our simulations of mixing on Ni, Pd, and Pt, materials in which EPC is expected to be significant owing to the large density of electron states at the Fermi level. We show here, however, that EPC is negligible in these materials and suggest that it can have only minor influence on other materials as well.

The relocation of atoms in materials induced by ion irradiation is called ion beam mixing.²⁰ In materials with dense cascades and low melting points a large fraction of the total mixing results from atom movement in a liquidlike region formed by the cascade.²¹ If the cooling of this liquid is en-

hanced by electron-phonon coupling the ion-beam mixing will be strongly reduced.¹² Thus ion mixing provides a valuable test of EPC models.

The mixing efficiency has been measured in a wide range of materials.²² A notable result of this work is that the mixing in Ni, Pd, and Pt is about a factor of 5 or more smaller than in Cu, Ag, and Au, respectively.^{22,23} Since these pairs of materials have similar atomic densities and masses, the purely ballistic aspects of mixing are virtually the same in the two groups. Alternative explanations for the different mixing value is that (i) the thermal spike is quenched in Ni, Pd, and Pt, but not in the noble metals, owing to strong electron-phonon coupling in the former group;¹³ and (ii) the higher melting temperatures (or cohesive energy) of Ni, Pd, and Pt diminishes the effects of thermal spikes.^{24,25} Since the correct interpretation of these experiments is vital for understanding cascade processes and evaluating current MD models, we examine the problem in detail, performing a direct comparison between experimental and simulated results of ion mixing in Ni, Pd, and Pt. Since we do not include EPC in our MD code, such a comparison provides a straightforward evaluation of its importance.

Ion beam mixing in Ni, Pd, and Pt has been measured accurately by several authors using marker layer experiments.^{22,23,26} One problem with interpreting the experiments is that even when thin impurity marker layers are employed, the type of tracer impurity can affect the results.²³ For self-atom mixing, therefore, one should in principle use isotopes, but short of this, tracer impurities that are as physically and chemically similar as possible to the host materials are preferred. Since Ni, Pd, and Pt form nearly ideal solutions with each other,²⁷ their combinations are well suited to obtain the elemental mixing efficiency. Hence we compare our simulations to the low-temperature data by Kim *et al.* of mixing in Ni(Pt) and Pt(Ni) systems²³ and to the data of Fenn-Tye and Marwick in the Pd(Pt) system.²⁶ These experiments all employed Kr beams at energies where subcascade overlap is negligible.²⁶

We performed additional mixing experiments on the materials to gain certainty that the tracer impurity mixing experiments represented self mixing. Here we investigated Ni markers in Pd and Pd markers in Ni since their cohesive properties are more similar to each other than to Pt,²⁷ which has been used as the tracer in previous experiments. Our

TABLE I. Simulated (sim.) and measured (exp.) values for the mixing efficiency Q .

Material	Beam	Q_{sim} ($\text{\AA}^5/\text{eV}$)	Q_{exp} ($\text{\AA}^5/\text{eV}$)
Ni	600 keV Kr	5.1 ± 0.4	4.8 ± 0.5^a
Ni	650 keV Kr	5.2 ± 0.4	5.0 ± 0.7^b
Pd	600 keV Kr	9.8 ± 0.8	8.4 ± 0.8^a
Pd	400 keV Kr	9.5 ± 0.8	9 ± 1^c
Pt	1 MeV Kr	14 ± 1	14 ± 2^b

^aPresent work.

^bReference 23.

^cReference 26.

experiments were carried out along the same lines as in Ref. 23, using secondary ion mass spectrometry (SIMS) to determine the marker layer widths. In Pd we grew two Ni marker layers at depths of 400 and 1400 \AA ; the depth between the two marker layers was used to calibrate the SIMS depth scale. For Ni a single Pd marker layer at 400 \AA was used. The calibration of sputtering time into depth in the SIMS measurements was done from the surface to the marker layer of the as-deposited sample. The SIMS results of mixing in Ni with Pd markers and Pd with Ni markers are given in Table I. As our values agree within the experimental uncertainties with the literature values, it is reasonable to assume that these values indeed represent self-atom mixing.

An additional consideration in comparing experiments with our simulations is the energy and mass of the irradiation particles. The heat spike mixing is easiest to interpret when the beam energy is sufficiently high that subcascades are formed and their overlap is negligible. In this case, the process causing mixing can be understood as follows. The incident ion travels mostly in a nearly straight path, but occasionally undergoes an energetic collision with a target atom. The recoil atom then initiates a local subcascade forming a heat spike and hence produces mixing.

This process is accurately simulated using two stages of molecular dynamics methods. Molecular dynamics range calculations²⁸ are employed to follow the motion of the implanted ion and obtain the number of primary recoils per incident ion as a function of energy, i.e., the primary recoil spectrum. Full molecular-dynamics simulations are then used to obtain the average atom relocation caused by the primary recoils of different energies. When subcascade overlap is negligible, integration of the primary recoil spectrum of the incident ion, weighted by the mixing caused by primary recoils, yields a mixing efficiency which directly corresponds to the experimental one.

The MD range calculation method presented in Ref. 28 was used to obtain the primary recoil spectrum $n(E)dE$ (the average number of primary recoils produced in a certain energy interval per implanted ion) in polycrystalline metals for Kr ions. Accurate *ab initio* repulsive potentials were used to ensure that the primary recoil spectrum is realistic.⁵

MD simulations of full collision cascades were used to obtain the mixing caused by self-recoils. To obtain a reliable picture of self-mixing at the highest energies, we had to simulate cascades at an energy where most of the cascades had broken down into subcascades. In Ni and Pd this

amounted to an energy of 100 keV and in Pt to 200 keV.

The square of the total atom displacements $R_{\text{sim}}^2(E) = \sum_i [r'_i - r_i^0]^2$ was obtained for selected recoil energies between 0.4 and 200 keV in each material (r_i^0 is the initial position of atom i and r'_i the position after the cascade has cooled down). The general computational principles used and the 0.4–10 keV simulations have been described in detail elsewhere.^{25,29} The 50–200 keV simulations were performed in the same manner as the lower-temperature runs, with cell sizes of up to 4 million atoms for the 200 keV Pt runs. We did not include any model of electron-phonon coupling in our simulations. Both the range and full cascade calculations employed SRIM96 electronic stopping powers to describe electronic energy loss of energetic ($E_{\text{kin}} > 10$ eV) atoms.³⁰

Previous studies have shown that the ion-beam mixing in heavy metals derives mostly from mixing in the liquidlike zone of the cascade.²⁵ Hence it is particularly sensitive to the melting point of the material.²⁹ Since the Pd and Pt embedded-atom method (EAM) potentials by Foiles³¹ do not reproduce the experimental melting point well, we modified these potentials to reproduce the experimental melting points to within 4%. By modifying the potentials only at separations smaller than the nearest-neighbor distance we ensured that the modification did not affect the equilibrium properties described well by the original potential.

At close separations all the EAM potentials were smoothly joined to the universal Ziegler-Bersack-Littmark interatomic repulsive potential³² to realistically describe strong collisions. The joining was calibrated by requiring that the final potential reproduces the experimental threshold displacement energy to within a few eV. The potentials were also found to be in good agreement with experimental high-pressure equations of state^{33,34} in the pressure regime below 10 GPa relevant in collision cascades.³⁵

In all materials, at least six 0.4, 2, and 10 keV cascades were simulated. In Ni and Pd additionally five 50 and 100 keV cascades and in Pt three 100 and 200 keV events were simulated. R_{sim}^2 was obtained for each energy as the average over R^2 for each individual event. Subcascade breakdown started to occur around 50 keV in Ni and Pd, but even at 100 keV many of the cascades still formed only one continuous liquid zone, although its shape was mostly quite elongated. The total amount of atom relocation at the same energy in the same material could differ by more than a factor of 2 between different events, emphasizing the need to obtain adequate statistics at each energy. Cascades which produced several liquid zones, or subcascades, usually exhibited much lower mixing values than cascades where only one, roughly spherical, continuous liquid was formed.³⁶ The liquid zones in the 50–200 keV events existed for about 10–30 ps, with the mixing increasing significantly over the first 5–10 ps. Since ballistic mixing occurs within the first few tenths of a picosecond, the mixing can be expected to indeed be sensitive to EPC cooling if it is present. The R_{sim}^2 results are given in Table II.

To enable interpolation between the R_{sim}^2 data points, a function $R^2(E)$ is fitted to the simulated data.³⁷ This function was constructed as follows. At low energies (≤ 10 keV) the mixing was of a pure heat spike character, and excellent fits

TABLE II. Simulated values for the total atom displacement R_{sim}^2 in Ni, Pd, and Pt.

Energy (keV)	R_{sim}^2 (Ni) (\AA^2)	R_{sim}^2 (Pd) (\AA^2)	R_{sim}^2 (Pt) (\AA^2)
0.4	205 ± 20	172 ± 24	166 ± 29
2.0	1800 ± 180	1860 ± 110	1470 ± 50
10.0	18300 ± 720	20500 ± 1600	18400 ± 1400
50.0	140000 ± 23000	242000 ± 25000	—
100.0	350000 ± 64000	474000 ± 32000	678000 ± 95000
200.0	—	—	2030000 ± 530000

to the simulated data were obtained using a simple power law with an exponent of exactly 1.5, i.e., $R^2(E) = aE^{3/2}$, where a is a fitted constant. At high energies, where cascades are completely broken down into subcascades, it is well known both experimentally and theoretically that the total atom relocation increases linearly with the nuclear damage energy E_{D_n} .²² We used the function

$$R^2(E) = a \frac{E^{3/2}}{b^{1/2} + E^{1/2}}, \quad (1)$$

which has both the desired low-energy and high-energy energy dependence, and only two fitting parameters a and b .³⁸

Using $R^2(E)$ obtained from the full MD simulations and the primary recoil spectrum $n(E)dE$ obtained from the range calculations, the total mixing efficiency caused by the 400–1000 keV Kr beam in each material is obtained using

$$Q_{\text{sim}} = \frac{\int_0^{E_0} R^2(E)n(E)dE}{6n_0E_{D_n}}, \quad (2)$$

where E_0 is the initial implantation energy, n_0 the atomic density and E_{D_n} the deposited nuclear energy of the Kr beam. This simulated mixing can be shown to be equivalent to the experimental one.^{21,25}

Since the marker layer is broadened during the irradiation, the mixing was calculated in a depth region 200 \AA above and below the initial location of the marker layer used in the experiments. We checked that the exact choice of this region, or the difference in stopping due to the presence of the marker layer did not have a significant effect on the results. The error estimates of the Q_{sim} data include statistical uncertainties of the primary recoil spectrum and the fit to the R_{sim}^2 data.

The calculation of the mixing in Ni is illustrated in Fig. 1. The figure shows the simulated R_{sim}^2 values as data points, and the fit of function (1) with a solid line. The dashed line indicates $Q'_{\text{sim}}(E)$ obtained from Eq. (2) by integrating from 0 to E . The final mixing $Q_{\text{sim}} = Q'_{\text{sim}}(600 \text{ keV})$. We see that most of the mixing derives from primary recoils with energies ~ 30 – 300 keV. Even though the number of such recoils is very much smaller than the number of lower-energy ones, they dominate the mixing because of the huge heat spike contribution in high-energy cascades.

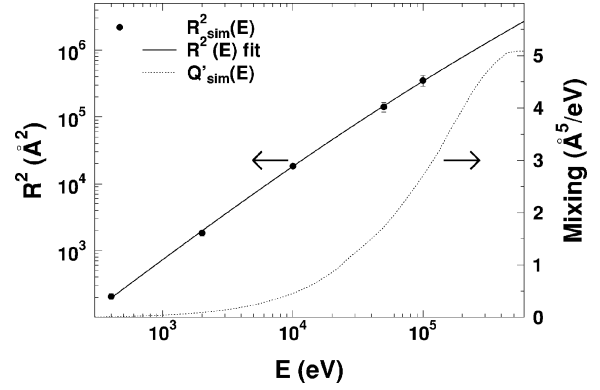


FIG. 1. Simulated R^2 values (circles), fit of the function $R^2(E)$ to the simulated data, and mixing $Q'(E)$ (dashed line). An excellent fit to the simulated data is obtained over about three orders of magnitude in both energy and mixing.

The mixing results are summarized in Table I. The experiments and simulations agree within the uncertainties in all the materials. Considering the uncertainties generally involved in the field²⁹ this can be considered remarkably good agreement. Most important is that we did not take into account the electron-phonon coupling in the simulations. Hence the good agreement between simulated and experimental mixing values shows that the effect of EPC on cascade development in Ni, Pd, and Pt cannot be as large as previously suggested. As the uncertainties of the MD simulations and experiments are of the order of 10–20% (Ref. 29) we cannot exclude the possibility that EPC might influence the mixing by this small factor, ~ 1.3 . This is dramatically less than the factors of ~ 3 – 10 suggested by most theoretical models. We thus conclude that the role of electron-phonon coupling in the mixing in Ni, Pd, and Pt is limited to $\sim 30\%$, and thus a small perturbation, at most, on cascade dynamics.

Our result is quite surprising when viewed against the predictions of theoretical models. These models are, however, based on equilibrium concepts whose validity is questionable in the highly localized and disordered state characteristic of cascades; one of the more recent EPC treatments in fact points out that no definite conclusions can be drawn on the magnitude of EPC.¹⁶ Our result is also supported by the recent observation by Smith *et al.* that simulations of low-energy (≤ 2 keV) mixing in Ni agrees better with experimental bilayer Ni mixing when electron-phonon coupling is not included,¹⁵ although thermal spike effects are small at these low energies (see Table II).

Traditionally EPC has been believed to be especially strong in Ni, Pd, and Pt, because of their electron structures, as noted above. Since we have now shown that it is not important in these metals, it is reasonable to assume it is not very important in most other metals. The method presented, however, provides for direct testing of this question in any material where mixing can be measured.

In conclusion, we have directly compared simulations and experiments of ion-beam mixing using no adjustable parameters or significant extrapolations. Simulations of cascades with energies up to 200 keV were performed. The primary

finding of this work is that electron-phonon coupling can play only a minor role in the dynamics of energetic collision cascades in Ni, Pd, and Pt.

The research was supported by the U.S. Department of Energy, Basic Energy Sciences, under Grant No. DEFG02-

91ER45439, and the Academy of Finland. Grants of computer time from the National Energy Research Computer Center at Livermore, California, the NCSA at Urbana-Champaign, Illinois, and the Center for Scientific Computing in Espoo, Finland, are gratefully acknowledged.

*Present address: Accelerator Laboratory, P.O. Box 43, FIN-00014 University of Helsinki, Finland. Electronic address: kai.nordlund@helsinki.fi.

¹D. J. Bacon, A. F. Calder, and F. Gao, *Radiat. Eff. Defects Solids* **141**, 283 (1997).

²R. S. Averback and T. Diaz de la Rubia, *Solid State Physics*, edited by H. Ehrenfest and F. Spaepen (Academic Press, New York, 1998), Vol. 51, p. 281.

³M. S. Daw, S. M. Foiles, and M. I. Baskes, *Mater. Sci. Rep.* **9**, 251 (1993).

⁴H. Balamane, T. Halicioglu, and W. A. Tiller, *Phys. Rev. B* **46**, 2250 (1992).

⁵K. Nordlund, N. Runeberg, and D. Sundholm, *Nucl. Instrum. Methods Phys. Res. B* **132**, 45 (1997).

⁶T. Diaz de la Rubia and G. H. Gilmer, *Phys. Rev. Lett.* **74**, 2507 (1995).

⁷T. Mattila and R. M. Nieminen, *Phys. Rev. Lett.* **74**, 2721 (1995).

⁸F. Gao and D. J. Bacon, *Philos. Mag. A* **75**, 1603 (1997).

⁹Y. Zhong, K. Nordlund, M. Ghaly, and R. S. Averback (unpublished).

¹⁰M. Ghaly, K. Nordlund, and R. S. Averback (unpublished).

¹¹C. P. Flynn and R. S. Averback, *Phys. Rev. B* **38**, 7118 (1988).

¹²M. W. Finnis, P. Agnew, and A. J. E. Foreman, *Phys. Rev. B* **44**, 567 (1991).

¹³I. Koponen, *J. Appl. Phys.* **72**, 1194 (1992).

¹⁴V. G. Kapinos and D. J. Bacon, *Phys. Rev. B* **53**, 8287 (1996).

¹⁵R. Smith, B. King, and K. Breadmore, *Radiat. Eff. Defects Solids* **141**, 425 (1997).

¹⁶I. Koponen, *Phys. Rev. B* **47**, 14011 (1993).

¹⁷K. Tappin, I. M. Robertson, and M. A. Kirk, *Philos. Mag. A* **70**, 463 (1994).

¹⁸J. L. Klatt, R. S. Averback, and D. Peak, *Appl. Phys. Lett.* **55**, 1295 (1989).

¹⁹M. Spaczér, A. Almazouzi, R. Schublin, and M. Victoria, *Radiat. Eff. Defects Solids* **141**, 349 (1997).

²⁰S. Matteson and M.-A. Nicolet, *Annu. Rev. Mater. Sci.* **13**, 339 (1983).

²¹T. Diaz de la Rubia, R. S. Averback, R. Benedek, and W. E. King, *Phys. Rev. Lett.* **59**, 1930 (1987).

²²See, e.g., B. M. Paine and R. S. Averback, *Nucl. Instrum. Methods Phys. Res. B* **7/8**, 666 (1985).

²³S.-J. Kim, M.-A. Nicolet, R. S. Averback, and D. Peak, *Phys. Rev. B* **37**, 38 (1988).

²⁴Y. T. Cheng, M. V. Rossum, M.-A. Nicolet, and W. L. Johnson, *Appl. Phys. Lett.* **45**, 185 (1984).

²⁵K. Nordlund, M. Ghaly, and R. S. Averback, *J. Appl. Phys.* **83**, 1238 (1997).

²⁶I. A. Fenn-Tye and A. D. Marwick, *Nucl. Instrum. Methods Phys. Res. B* **18**, 236 (1987).

²⁷A. R. Miedema, *Philips Tech. Rev.* **36**, 217 (1976).

²⁸K. Nordlund, *Comput. Mater. Sci.* **3**, 448 (1995).

²⁹K. Nordlund *et al.*, *Phys. Rev. B* **57**, 7556 (1998).

³⁰J. F. Ziegler (private communication).

³¹S. M. Foiles, *Phys. Rev. B* **32**, 3409 (1985).

³²J. F. Ziegler, J. P. Biersack, and U. Littmark, *The Stopping and Range of Ions in Matter* (Pergamon, New York, 1985).

³³H. K. Mao, P. M. Bell, J. W. Shaner, and D. J. Steinberg, *J. Appl. Phys.* **49**, 3276 (1978).

³⁴V. N. Antonov, V. Y. Milman, V. V. Nemoshkalenko, and A. V. Zhalko-Titarenko, *Z. Phys. B* **79**, 233 (1990).

³⁵R. S. Averback, *J. Nucl. Mater.* **216**, 49 (1994).

³⁶Animations illustrating the development of the heat spike are available on the World Wide Web in <http://beam.helsinki.fi/~knordlund/casc/>, and in AIP Document No. E-PAPS: E-PRBMDO-57-R32822. E-PAPS document files may be retrieved free of charge from our FTP server (<http://www.aip.org/epaps/epaps.html>) or from <ftp.aip.org> in the directory /epaps/. For further information: e-mail: PAPS@aip.org or fax: 516-576-2223.

³⁷P. R. Bevington, *Data Reduction and Error Analysis for the Physical Sciences* (McGraw-Hill), New York, 1992).

³⁸Both MDRANGE and full MD simulations showed that E_{D_n} depends linearly on E in the presently used energy range, whence we can use E rather than E_{D_n} in the function.